JOURNAL OF PROPULSION AND POWER
Vol. 26, No. 2, March–April 2010

Core Noise Diagnostics of Turbofan Engine Noise Using Correlation and Coherence Functions

Jeffrey Hilton Miles*
NASA John H. Glenn Research Center at Lewis Field, Cleveland, Ohio 44135

DOI: 10.2514/1.42980

Cross-correlation and coherence functions are used to look for periodic acoustic components in turbofan engine combustor time histories, to investigate direct and indirect combustion noise source separation based on signal propagation time delays, and to provide information on combustor acoustics. This investigation uses a combustor pressure sensor and a far-field microphone at 130° to study the change in propagation time to the far field of the direct and indirect combustion noise signal using a generalized cross-correlation function. Results are presented as a function of the cutoff frequency of the low-pass filter used to create the generalized cross-correlation function and engine operating condition. The filtering procedure used produces no phase distortion. As the low-pass-filter frequency is decreased, the travel time increases. The indirect combustion noise signal travels more slowly, because the entropy in the combustor moves with the flow, which has a low velocity. The indirect combustion noise signal travels at acoustic velocities after reaching the turbine and being converted into an acoustic signal. The direct combustion noise is always propagating at acoustic velocities. This is in agreement with previous investigations of delay times using a cross-spectrum phase-angle method with unfiltered signals that found indirect combustion noise to be in the 0–200 Hz frequency range and the direct combustion noise to be in the 200–400 Hz frequency range. Similar results obtained using the cross-spectrum phase-angle method with filtered signals are also shown. These results show that the low-pass filtering can be used with the cross-correlation function to separate this type of dependent source and confirm the cross-spectrum results. Although the results are based on a set of static engine tests conducted for one specific dual-spool turbofan engine configuration, they may lead to a better idea about the acoustics in the combustor turbine-tailpipe system and may help develop and validate improved reduced-order physics-based methods for predicting turbofan engine core noise.

Nomenclature

B_e	=	resolution bandwidth, Hz, $1/T_d = r_s/N = 2$ Hz
c_c	=	combustor-region speed of sound, m/s
c_o	=	ambient speed of sound, m/s
D	=	propagation time delay or lag, s
f_c	=	upper frequency limit, $1/2\Delta t = r_s/2$, Hz (32,768 Hz)
f_L	=	cutoff frequency of low-pass filter
L_c	=	combustor-region length, m
L_y	=	number of frequencies, $f_c/\Delta f = N/2$ (16,384)
M_c	=	combustor-region Mach number
N	=	segment length, number of data points per segment (32,768)
n_o	=	number of overlapped data segments/blocks
n_s	=	number of disjoint (independent) data segments/blocks, $B_e T_{\text{total}} \approx 128$
P_I	=	confidence-interval percent value used to calculate coherence threshold
$\Re$	=	gas constant, 8314 J/k mol K
R_x	=	autocorrelation function
R_{xy}	=	cross-correlation function
r	=	microphone radial location, m (30.48 m)
r_s	=	sample rate, samples/s (65,536)
T_c	=	temperature in combustor, K
$T_d(i)$	=	record length of segment i, N/r_s, 0.5 s
T_{total}	=	total record length, s ($\approx$70 s)
t	=	time, s
v_s	=	combustor-region flow convection velocity, m/s
W	=	molecular weight of air, 28.97 kg/k mol
x	=	time-dependent signal
y	=	time-dependent signal
γ	=	ratio of specific heats, 1.4
γ^2_{nn}	=	magnitude squared coherence function of noise
γ^2_{xy}	=	magnitude squared coherence function of signals x and y
Δf	=	frequency step, $1/T_d = r_s/N$, Hz (2 Hz)
Δt	=	sampling interval, $1/r_s$ (1/65,536), s
$\Delta\tau$	=	combustor-region time delay, s
$\Delta\tau(f_L)\|_{\text{peak}}$	=	measured combustor convection time delay less 90, s
ρ_{xy}	=	cross-correlation coefficient
τ	=	time, s
τ_a	=	combustor-region acoustic wave travel time, s
τ_d	=	direct combustion noise-signal travel time, s
τ_{duct}	=	noise-signal travel time in the duct, s
τ_i	=	indirect combustion noise-signal travel time, s
τ_s	=	combustor-region entropy travel time, s

Subscript

i	=	running segment index

Presented as Paper 1237 at the 47th AIAA Aerospace Sciences Meeting, Orlando, FL, 5–8 January 2009; received 29 December 2008; revision received 12 October 2009; accepted for publication 27 October 2009.

*Aerospace Engineer, Acoustics Branch, 21000 Brookpark Road. Associate Fellow AIAA.

I. Introduction

THE study of turbofan engine core noise is conducted to develop noise diagnostic tools, noise prediction schemes, and noise reduction technologies. Combustion noise, both direct and indirect, is an important contributor to low-frequency core noise. Combustion noise is difficult to study because hydrodynamic and acoustic pressure fluctuations are intermixed at the source location. In addition, much of the far-field noise is not correlated with the combustor and/or turbine-tailpipe internal noise. However, the part that is correlated can be studied using signal cross-correlation functions and

coherence functions. The goal of this study is to improve understanding of the acoustics in combustors that will ultimately enable development of improved reduced-order physics-based methods for predicting core noise.

This paper compares time-domain and spectral-domain methods using cross-correlation functions and coherence functions. The methods are applied to data from a dual-spool TECH977 turbofan engine. Acoustic data from the same TECH977 engine test program are discussed by Miles [1,2], Mendoza et al. [3], Weir and Mendoza [4], Schuster [5], Royalty and Schuster [6], Dougherty and Mendoza [7], Weir [8], and Hultgren and Miles [9]. The research discussed is an extension of the study of the combustion noise of the TECH977 engine conducted by Miles [1,2] using a coherent output-power spectral-domain coherence-function approach.

The core noise components of the dual-spool turbofan engine were separated by Miles [1,2] using coherence functions. A source-location technique was used that adjusted the time delay between the combustor pressure-sensor signal and the far-field microphone signal to maximize the coherence and remove as much variation of the phase angle with frequency as possible. For the 130° microphone, a 90.03 ms time shift worked best for the frequency band from 0–200 Hz, whereas a 86.98 ms time shift worked best for the frequency band from 200–400 Hz. Hence, the 0–200 Hz band signal took more time than the 200–400 Hz band signal to travel the same distance. This suggests that the 0–200 Hz coherent cross-spectral density band is partly due to indirect combustion noise attributed to entropy fluctuations, which travel at a low-flow velocity in the combustor until interactions with the turbine pressure gradient produce indirect combustion noise. The indirect noise source was studied by Pickett [10], Cumpsty and Marble [11,12], Cumpsty [13], Gliebe et al. [14], and Mani [15]. The signal in the 200–400 Hz frequency band is attributed mostly to direct combustion noise. The method discussed herein is successful because acoustic and temperature fluctuations caused by hot-spot convection were found by Miles et al. [16] to be related by a linear transfer function that includes a convective time delay. This experiment involved the measurements of pressure and temperature disturbances in a long tube connected to a combustor. This linear connection of entropy and pressure fluctuations implies that direct and indirect combustion noise are dependent.

Cross-correlation functions are discussed in standard signal-processing texts such as those by Bendat and Piersol [17–19], Childers and Durling [20], Kay [21], Stearns and David [22], and Candy [23]. Computational methods are discussed by Childers and Durling [20], Kay [21], and Stearns and David [22]. The cross-correlation function was used to detect periodic signals in noise by Lee et al. [24]. White [25] used the cross-correlation function and filters to look for propagation time delays in a system with periodic signals.

Cross-correlation functions were used by Karchmer and Reshotko [26] to study propagation time delays from a AVCO-Lycoming YF–102 turbofan engine combustor to a far-field microphone located at a 120° polar angle. Combustion noise below 250 Hz was attributed to an indirect combustion noise source. Cross-correlation functions were obtained using low-pass-filtered signals to remove frequencies above 1600 or 240 Hz. Karchmer [27] presented additional results. In particular, cross-correlation functions were shown again using low-pass-filtered signals to remove frequencies above 240 Hz. Reshotko and Karchmer [28] presented similar test results for the Pratt & Whitney JT15D turbofan engine. Combustion noise below 250 Hz was attributed a direct combustion noise source. Cross-correlation functions were shown using signals that were low-pass-filtered at 240 Hz. Mathews et al. [29] studied propagation time delays from a Pratt & Whitney JT8D-109 engine combustor to the far field using the cross-correlation function and attributed the noise source to the combustor. Their report attributed the noise to direct combustion noise and cited calculations that indicated that indirect combustion noise was much lower than direct combustion noise. Shivashankara [30], using the cross-correlation function, studied propagation time delays from an auxiliary power unit. Combustion noise below 400 Hz was attributed to a direct combustion noise source. Cross-correlation functions were shown using signals filtered to remove frequencies above 1000 Hz. More recently, Harper-Bourne et al. [31] used the cross-correlation function to study the combustion noise of a turbofan demonstrator engine. The engine study program used internal and external sensors. The method revealed delay times from the internal combustor sensor to the far-field microphone, even though the correlated signal contained both periodic and random components. In addition, indirect combustion noise has been investigated numerically and with model-scale experiments by Schemel et al. [32], Richter et al. [33], and Bake et al. [34–36].

The fundamental premise of this paper is that filtering to remove frequencies above 400 Hz leaves the combined direct and indirect combustion noise unchanged in the signal. Filtering to remove frequencies above 200 Hz leaves the indirect combustion noise mostly unchanged. In addition, the low-pass filters are designed to eliminate phase-angle modifications and to leave the signal delay time identified as the location of peak of the correlation function of random noise at the same time value.

Fundamental to the interpretation of the results presented is that entropy waves or hot spots travel at the flow velocity, which is only a fraction of the speed of sound. According to Hill and Peterson [37], the average axial velocity of the combustor reactants, v_s, is of the order of 30 m/s. The speed of sound in a combustor, c_c, is generally calculated based on the assumption that the air is a perfect gas [37–39]:

$$c_c = \sqrt{\gamma \Re T_c / W} \tag{1}$$

As reported by Hill and Peterson [37], typical turbine inlet temperatures are of the order of 1600 K. Consequently, the speed of sound c_c is of the order of 800 m/s. Thus, the Mach number of the hot spots is about 0.0375. This assumption is not a practical limitation to the present investigation. However, the use of the perfect-gas assumption is subject to certain limitations, as pointed out by Barrett and Suomi [40] and Cramer [41], such as the assumption that the incremental pressure due to the sound wave is very small compared to the static pressure of the medium; the frequencies are low so that γ is independent of frequency.

This paper examines signals at the 130° microphone. Engine operating conditions of 48, 54, 60, and 71% of maximum power are evaluated. Results are presented for an unfiltered condition and after low-pass filtering to remove frequencies above 400, 300, 200, 150, and 100 Hz using a filtering procedure that has no phase distortion. The idea of prefiltering the signals before doing a cross correlation is discussed by Knapp and Carter [42], Carter [43], and Scarbrough et al. [44], and the resulting function is identified as a generalized cross-correlation (GCC) function. However, the problem of phase distortion introduced by the filters used in creating the GCC function is not discussed in these papers. In addition, for the 400 and 150 Hz low-pass filter, aligned coherence-function and coherent-combustion power results are shown using a time shift of 86.98 and of 90.03 ms. In the next section, the engine noise data and analysis are presented.

II. Engine Noise Data and Analysis

A. Engine Test Data

The static engine test was conducted at Honeywell's San Tan outdoor acoustic test facility. A polar array of 32 ground-plane microphones was used. Each B&K 4134 microphone in an inverted stand with a 7-mm ground spacing was placed on a 100 ft radius. The microphones were positioned from 5 to 160° (relative to the inlet) in 5° increments. The microphone at 130° was used in this study.

The dual-spool turbofan engine has a direct-drive wide chord fan connected by a long shaft to the low-pressure turbine spool and a high-pressure compressor connected by a concentric short shaft to the turbine high-pressure spool. The fan diameter is 34.2 in. The combustor design is a straight throughflow annular geometry with 16 fuel nozzles and 2 igniters. One of the igniters is replaced by a pressure transducer, which is identified herein as CIP1. The dependent source-separation technique used to identify direct and

indirect combustion noise uses data from the CIP1 transducer and a far-field microphone.

The data acquisition system had a sampling rate of 65,536 Hz and a sampling duration of roughly 70 s. This permitted data reduction using 254 overlapped ensemble averages at a bandwidth resolution of 2 Hz. Further signal estimation parameters are shown in Table 1.

B. Correlation Functions

The autocorrelation function describes the general dependence of the values of data at one time on the value at another time. The autocorrelation function is

$$R_{xx}(\tau) = \lim_{T\to\infty} \frac{1}{T} \int_0^T x(t)x(t+\tau)\,\mathrm{d}t \tag{2}$$

The cross-correlation function describes the general dependence of the values of one set of data at one time on the value of another set of data at another time. The cross-correlation function is

$$R_{xy}(\tau) = R_{yx}(-\tau) = \lim_{T\to\infty} \frac{1}{T} \int_0^T x(t)y(t+\tau)\,\mathrm{d}t \tag{3}$$

Note that the cross-correlation function is not symmetric in time about zero.

The normalized cross-correlation function known as the cross-correlation-function coefficient (normalized cross-covariance function) used herein to plot the cross-correlation functions is defined as

$$\rho_{xy}(\tau) = \rho_{yx}(-\tau) = \frac{R_{xy}(\tau)}{\sqrt{R_{xx}(0)R_{yy}(0)}} \tag{4}$$

by Bendat and Piersol [18,19]. Although the total cross-correlation functions are calculated, only the positive time delay is shown.

C. Digital Filtering

Digital filter parameters for the three section low-pass filters used herein are shown as a function of cutoff frequency f_L in Tables 2–6, where, for $i = 1$, 2, and 3,

$$A_i(z) = 1 + a_i(1)z^{-1} + a_i(2)z^{-2}$$
$$B_i(z) = b_i(0) + b_i(1)z^{-1} + b_1(2)z^{-2}$$

and the transfer function of the linear digital filter section i is $H_{i(z)} = A_{i(z)}/B_{i(z)}$. The 100, 200, 300, and 400 Hz low-pass filters used herein are three-section Butterworth filters. Filter design was done using bilinear transformation following a method described by Stearns and David [22]. These filter parameters are given in Tables 2 and 4–6.

To see if the results depended on the filter design approach, a non-Butterworth filter was used as a 150 Hz filter, with coefficients shown in Table 3. For the first section, this filter uses the second-section filter values of the 300 Hz filter shown in Table 5. For the second and third section, this filter uses the third-section filter values of the 300 Hz filter shown in Table 5. The 150 Hz filter has a larger transition band than a properly designed Butterworth filter.

To make certain that the filters introduce no phase-angle modification, the filter for each segment is applied to the forward time series and then again with the time reversed. The time-series reversal is then removed before processing the next segment or quitting. This procedure is discussed by Kormylo and Jain [45] and by Hamming [46]. Note that the effective filter function is the square of the absolute value of the filter function designed.

Table 1 Spectral estimate parameters

Parameter	Value
[0.5ex] segment length (data points per segment) N	32,768
Sample rate r_s, samples/s	65,536
Segment length $T_d = N/r_s$, s	0.500
Sampling interval $\Delta t = 1/r_s$, s	1/65,536
Bandwidth resolution $B_e = \Delta f = 1/T_d = r_s/N$, Hz	2.0
Upper frequency limit $f_c = 1/2\Delta t = r_s/2$, Hz	32,768
Number of frequencies $Ly = f_c/\Delta f = N/2$	16,384
Propagation time delay/lag ($T = 9°$C, $r = 30.48$ m) $D = 5\,927/65\,536$, s	0.09044
Number of independent samples n_s	128
Overlap	0.50
Sample length, s	70

Table 2 100 Hz low-pass-filter parameters

Parameter	Values		
$A_1(z)$	−1.994957877158	0.995049566793	——
$B_1(z)$	0.000022922409	0.000045844817	0.000022922409
$A_2(z)$	−1.986441602897	0.986532901119	——
$B_2(z)$	0.000022824555	0.000045649111	0.000022824555
$A_3(z)$	−1.981557756270	0.981648830027	——
$B_3(z)$	0.000022768439	0.000045536878	0.000022768439

Table 3 150 Hz low-pass-filter parameters

Parameter	Values		
$A_1(z)$	−1.959329632211	0.960140349842	——
$B_1(z)$	0.000202679408	0.000405358816	0.000202679408
$A_2(z)$	−1.945140180302	0.945945026722	——
$B_2(z)$	0.0002012116a05	0.000402423210	0.000201211605
$A_3(z)$	−1.945140180302	0.945945026722	——
$B_3(z)$	0.000201211605	0.000402423210	0.000201211605

Table 4 200 Hz low-pass-filter parameters

Parameter	Values		
$A_1(z)$	−1.989758186880	0.990124031531	——
$B_1(z)$	0.000091461163	0.000182922325	0.000091461163
$A_2(z)$	−1.972884422898	0.973247165073	——
$B_2(z)$	0.000090685544	0.000181371087	0.000090685544
$A_3(z)$	−1.963272029823	0.963633004625	——
$B_3(z)$	0.000090243701	0.000180487401	0.000090243701

Table 5 300 Hz low-pass-filter parameters

Parameter	Values		
$A_1(z)$	−1.984402564179	0.985223656312	——
$B_1(z)$	0.0002052730330	0.000410546067	0.000205273033
$A_2(z)$	−1.959329632211	0.960140349842	——
$B_2(z)$	0.000202679408	0.000405358816	0.000202679408
$A_3(z)$	−1.945140180302	0.945945026722	——
$B_3(z)$	0.000201211605	0.000402423210	0.000201211605

Table 6 400 Hz low-pass-filter parameters

Parameter	Values		
$A_1(z)$	−1.978892639460	0.980348696212	——
$B_1(z)$	0.000364014188	0.000728028376	0.000364014188
$A_2(z)$	−1.945778355457	0.947210046928	——
$B_2(z)$	0.000357922868	0.000715845735	0.000357922868
$A_3(z)$	−1.927159619380	0.928577611302	——
$B_3(z)$	0.000354497980	0.000708995961	0.000354497980

D. White-Noise Results

To demonstrate the filtering process, a study was conducted using white noise generated by use of a Mersenne Twister random number

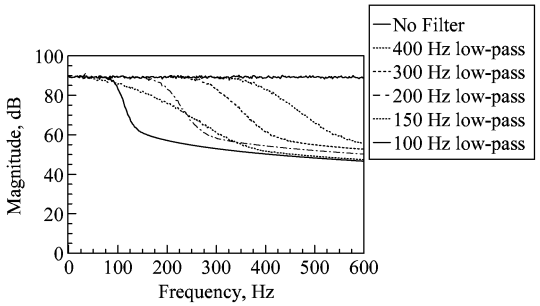

Fig. 1 Low-pass filters acting on random noise.

generator [47]. Figure 1 shows the effect of each filter on the signal amplitude.

Figure 2 shows cross-correlation functions generated using random-number-generated white noise and random-number-generated white noise displaced by $D_T = 86.98$ ms. Each plot has the cross-correlation function of the unfiltered signals and the signals filtered by the 100 Hz low-pass filter. Figures 2a–2d have the results

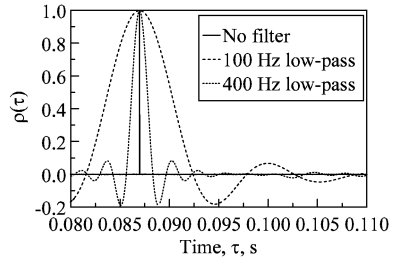

a) 100 and 400 Hz low-pass filter

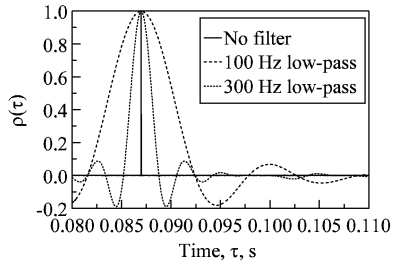

b) 100 and 300 Hz low-pass filter

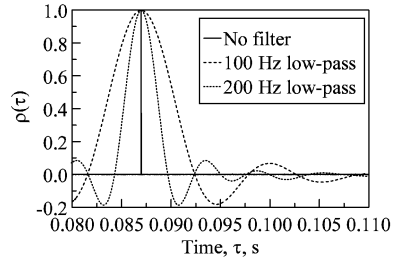

c) 100 and 200 Hz low-pass filter

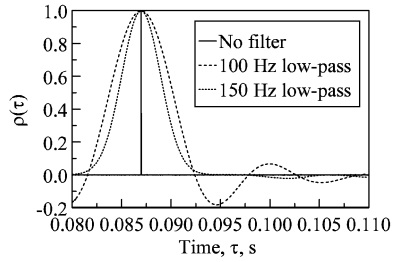

d) 100 and 150 Hz low-pass filter

Fig. 2 Cross-correlation with no filter and various low-pass filters of white noise displaced by $D_T = 5700/65,536 = 86.9751$ ms.

of the 400, 300, 200, and 150 Hz low-pass filters, respectively. The location of the peak value is constant, independent of the filter design. The width of the peak increases as the filter design frequency is reduced.

E. Coherence Threshold

A minimum threshold of the magnitude squared coherence, γ^2_{nn}, was obtained using the $P_I =$ percent confidence interval, as discussed by Carter [48,49], Halliday et al. [50], and Brillinger [51]. This threshold is given by

$$\gamma^2_{nn} = 1 - (1 - P_I)^{1/(n_s - 1)} \tag{5}$$

and represents the coherence of two independent time series, calculated using an average of n_s independent finite length sample segments.

Miles [52] showed that instead of relying on the confidence interval given by Eq. (5), which is based on a statistical theory, to obtain a threshold value for $\gamma^2_{nn}(f)$, one can use a deliberately unaligned time history to create the threshold value. If one of the time histories is shifted by a time delay more than the segment/block length $T_d = N/r_s$, then the two time histories are totally independent unless tones are present. This deliberate decorrelation establishes a coherence threshold and also identifies any tones in the signals. Shifting the signals by this time delay removes the coherence of random noise (identified frequently as broadband noise) but leaves the coherence of periodic functions (identified frequently as tones). Miles [52] found out that replacing n_s with n_o in Eq. (5), where n_o is the number of overlapping segments, gives a good estimate of the coherence squared noise threshold $\gamma^2_{nn}(f)$. Thus, for a 95% confidence interval, the noise floor is $\gamma^2_{nn} = 0.012$ ($n_o = 254$), where the number of overlapped averages is used, rather than the number of independent averages.

III. Results

A. Cross-Correlation with and Without Filtering

The sequence of low-pass filters, discussed in the previous section, is applied to the combustor pressure-transducer signal and far-field

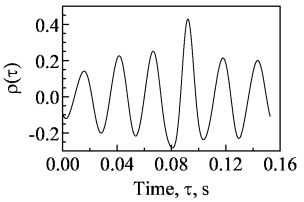

a) 100 Hz low-pass filter

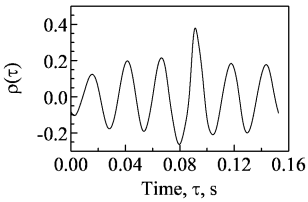

b) 150 Hz low-pass filter

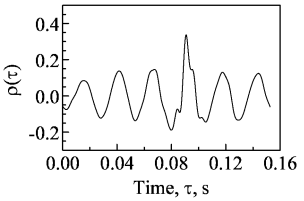

c) 200 Hz low-pass filter

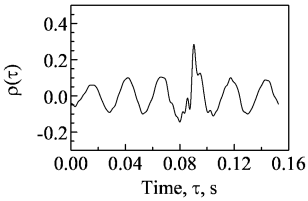

d) 300 Hz low-pass filter

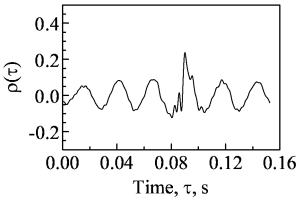

e) 400 Hz low-pass filter

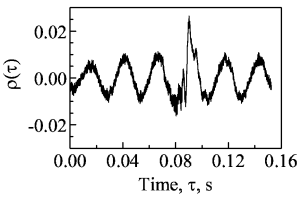

f) No filter

Fig. 3 Normalized cross-correlation function for turbofan engine operating at a setting of 48% maximum power.

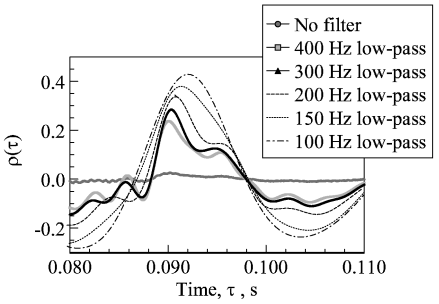

a) 100-400 Hz low-pass filters

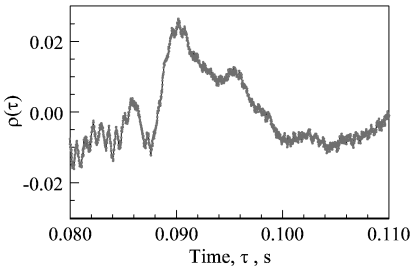

b) No filter

Fig. 4 Normalized cross-correlation calculated at setting of 48% maximum power in region of peak values.

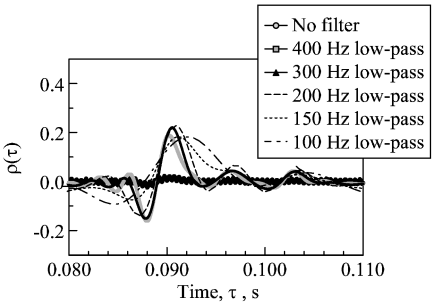

a) 100-400 Hz low-pass filters

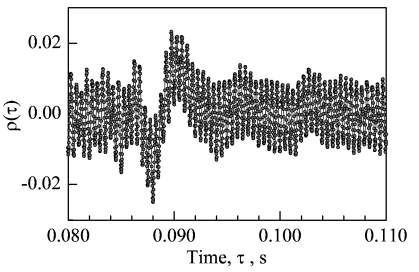

b) No filter

Fig. 6 Normalized cross-correlation at setting of 54% maximum power in region of peak values.

microphone signal. The signal resulting from using the 400 Hz low-pass filter contains both indirect and direct combustion noise. By applying further low-pass filters in the sequence (i.e., 300, 200, 150, and 100 Hz), the resulting signal will have a decreasing amount of direct combustion noise. The signal resulting from using the 100 Hz low-pass filter contains mainly indirect combustion noise.

The cross-correlation functions between the microphone at 130° and the combustor pressure sensor are presented in Figs. 3–10. Figures 4, 6, 8, and 10 show the cross-correlation functions in the time region from 80 to 100 ms, which contain the peak value. The left side of the peak is determined by the direct combustion noise, which moves at acoustic speed along its full path. The right side of the peak in the region is controlled by the indirect combustion noise, which initially propagates with the mean flow velocity.

The combustion noise spectrum has a limited frequency range. For this particular engine, this limit is about 400 Hz. Figure 2 shows that the cross correlation of two band-limited signals is smeared in the time domain. Consequently, one would expect to see a cross-correlation function with two smeared peaks here. Examination of the unfiltered cross-correlation function for the 48% of maximum power operating condition in Figs. 3f and 4b shows that this is the case. However, as the low-pass-filter cutoff frequency is decreased,

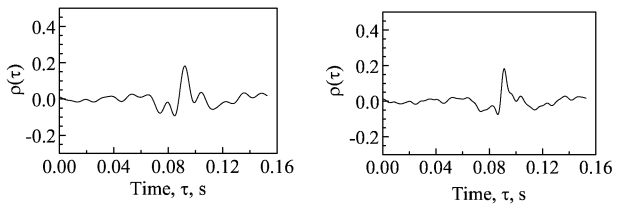

a) 100 Hz low-pass filter b) 150 Hz low-pass filter

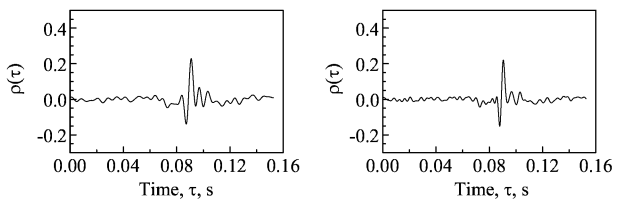

c) 200 Hz low-pass filter d) 300 Hz low-pass filter

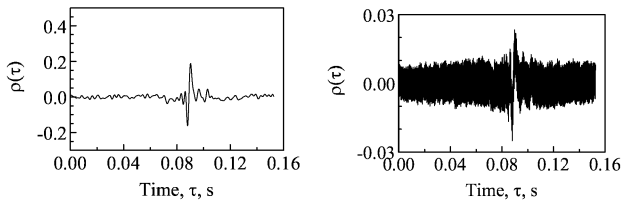

e) 400 Hz low-pass filter f) No filter

Fig. 5 Normalized cross-correlation function for turbofan engine operating at a setting of 54% maximum power.

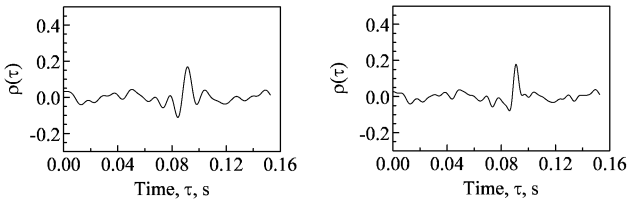

a) 100 Hz low-pass filter b) 150 Hz low-pass filter

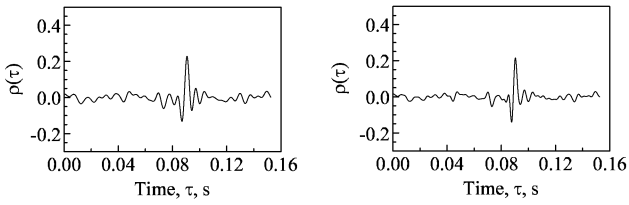

c) 200 Hz low-pass filter d) 300 Hz low-pass filter

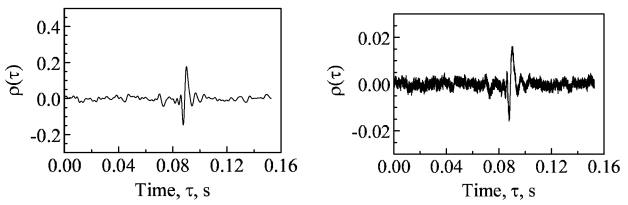

e) 400 Hz low-pass filter f) No filter

Fig. 7 Normalized cross-correlation function for turbofan engine operating at a setting of 60% maximum power.

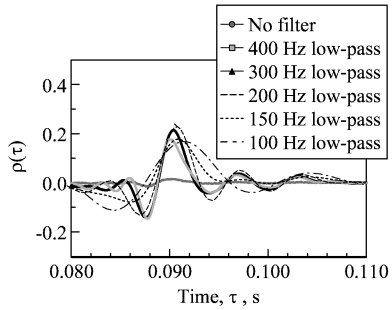

a) 100-400 Hz low-pass filters

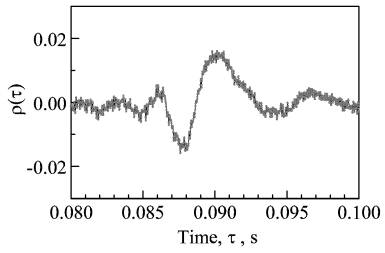

b) No filter

Fig. 8 Normalized cross-correlation calculated at setting of 60% maximum power in region of peak values.

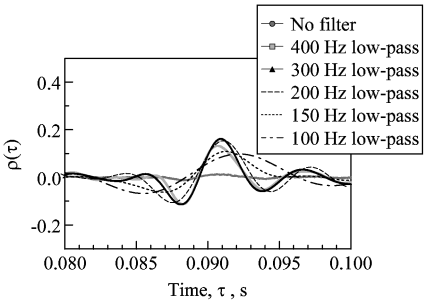

a) 100-400 Hz low-pass filters

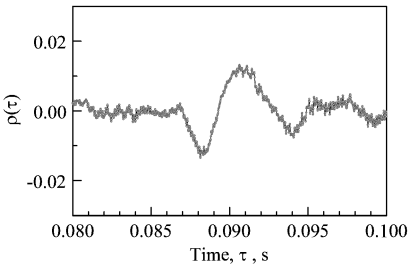

b) No filter

Fig. 10 Normalized cross-correlation calculated at setting of 71% of maximum power in region of peak values.

more direct combustion noise, which controls the left side of the peak, is removed and the temporal smearing is increased. For low-pass filters with a cutoff frequency less than 150 Hz, one sees only a single peak (Fig. 4a). In addition, the location of the double-peak or single-peak maximum value shifts to larger time delays as the low-pass-filter cutoff frequency is decreased. The no-filter case and the cases filtered with the 200–400 Hz low-pass filters show a first peak near 90 ms and a second smaller peak near 95 ms. The peak using the 100 Hz low-pass filter occurs at 92 ms.

At the three higher operating conditions, the two-peak phenomena are not observed in cross correlations made using the combustor pressure sensor with the 130° microphone; only a single-peak cross-correlation is observed. The reason that only a single peak is detected is not clear, but it is possible that the relative amount of indirect combustion noise in the signal is decreased, thus making its detection as a discrete peak more difficult at these three higher power settings. Another possibility is that the ripple that is observed at the 48% operating condition is due to a convective entropy feedback mechanism that enhances the indirect combustion noise signal for this case. However, in all cases, the single peak or the left peak, where a double peak occurs, shifts to the right as the low-pass-filter cutoff frequency is decreased.

The resulting delay time values of the peak are shown in Table 7. For the cases in which no filter was used or the case in which the 400 Hz low-pass filter was used, this time corresponds to about 90 ms. Peak values of the normalized cross-correlation function are shown in Table 8.

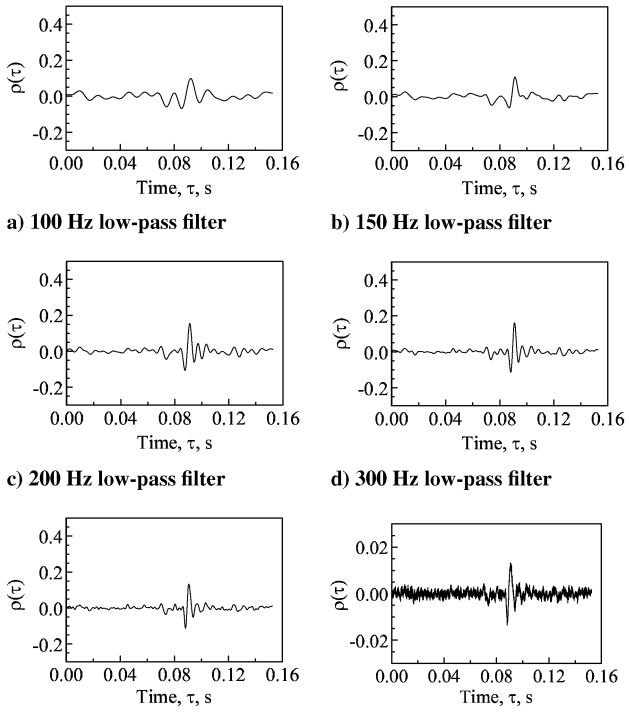

a) 100 Hz low-pass filter

b) 150 Hz low-pass filter

c) 200 Hz low-pass filter

d) 300 Hz low-pass filter

e) 200 Hz low-pass filter

f) No filter

Fig. 9 Normalized cross-correlation function for turbofan engine operating at a setting of 71% of maximum power.

B. Generalized Cross-Correlation Method

The desire to use the GCC method and to prefilter the signals before doing a cross correlation as discussed by Knapp and Carter [42], Carter [43], and Scarbrough et al. [44] comes from a need to accentuate the signal at those frequencies at which the signal-to-noise ratio is the highest. The prefiltering used herein is designed to serve a different objective. It is done to separate the direct combustion noise source, which produces waves always propagating at acoustic speeds, from the indirect combustion noise source, which produces waves that take longer to reach the far field, since they spend time moving with the flow velocity in the combustor.

To provide the baseline acoustic propagation speed, the unfiltered cross-correlation function was calculated. It is shown for the 48% maximum power case in Figs. 3f and 4b, for the 54% maximum power case in Figs. 5f and 6b, for the 60% maximum power case in Figs. 7f and 8b, and for the 71% maximum power case in Figs. 9f and 10b. These plots show cross-correlation functions with varying degrees of roughness or high-frequency modulation that is removed by low-pass filtering.

Figure 11 shows the aligned unfiltered coherence between the far-field microphone at 130° and the combustor sensor at four power setting. The 48% maximum power case shown in Fig. 11a has a narrow peak near 1346 Hz. The 54% maximum power case shown in Fig. 11b has a broad peak near 1350 Hz. These peaks may be related to a longitudinal instability mode in the engine core. Figures 11a–11d

Table 7 Time delays at peak of cross correlation of 130° microphone signal and CIP1 combustor pressure signal, ms

Engine power level	No filter	Low pass 400 Hz	Low pass 300 Hz	Low pass 200 Hz	Low pass ≈150 Hz	Low pass 100 Hz
48%	90.18	90.07	90.33	90.76	91.34	92.06
54%	89.74	90.19	90.52	90.90	91.16	92.12
60%	90.13	90.07	90.38	90.71	90.85	91.46
71%	90.62	90.67	90.91	91.08	91.25	92.16

Table 8 Peak values of normalized cross-correlation function of 130° microphone signal and CIP1 combustor pressure signal

Engine power level	No filter	Low pass 400 Hz	Low pass 300 Hz	Low pass 200 Hz	Low pass ≈150 Hz	Low pass 100 Hz
48%	0.026	0.237	0.284	0.337	0.379	0.429
54%	0.023	0.188	0.220	0.228	0.182	0.182
60%	0.016	0.177	0.215	0.228	0.178	0.169
71%	0.013	0.132	0.162	0.154	0.109	0.098

also show tones related to turbofan engine rotating shaft speeds. The longitudinal instability mode vanishes at higher power settings, but the coherence of the shaft speed tones increases in magnitude at higher power settings. The low-pass filtering removes these signals and provides smooth cross-correlation function free of high-frequency modulation.

C. Tones and the Coherence Threshold

The method of aligned and unaligned coherence presented by Miles [52] is extended in this paper to include cross-correlation functions. Aligned and unaligned cross-correlation and coherence functions are calculated using signals unaligned by 2.74 sample segment lengths ($D_T = 2.74 \cdot T_d = 1.37$ s). The presence of tones is clearly observable in the cross-correlation functions.

Figure 12 shows the unaligned coherence function between the microphone at 130° and the combustor pressure sensor CIP1 at four power settings. The signal processing is done using signals low-pass-filtered at 400 Hz, unaligned by 2.74 sample segment lengths ($D_T = 2.74 \cdot T_d = 1.37$ s) to obtain measured coherence noise floor and to observe tones. The measured noise floor and the statistical noise floor are in good agreement. Tones are tabulated in Table 9. The tone at 18 Hz occurred at all power settings. In Table 9 the tones at 354, 380, and 398 Hz are related to rotating shaft speeds and not due to a combustion noise source.

Figure 13 shows the corresponding unaligned cross-correlation functions. The tone at 18 Hz has a period of $T = 1/18 = 55$ ms. This wave structure is shown in Fig. 13 at each power setting. This wave is modulated by waves with periods of 2 to 10 ms.

D. Filtering to Remove Frequencies Greater than 400 Hertz

Miles [1,2] has shown that the cross-spectrum phase angle of unfiltered signals can be used to separate direct and indirect combustion noise. In this section, it is shown that the method works for the signals that are low-pass-filtered at 400 Hz. Only the results at 48% of maximum power are shown.

Figure 14 shows that the phase angle in the 200–400 Hz region (direct noise source region) is flat if a 86.98 ms time delay is removed. Figure 15 shows that the phase angle in the 0–200 Hz region (indirect noise source region) is flat if a 90.03 ms time delay is removed. This yields a 3.05 ms time delay between the direct combustion noise acoustic signal and the indirect combustion noise acoustic signal.

Figures 14 and 15 show that the ripple in the cross-correlation function (panel a) corresponds to the peak in the coherence function near 36 Hz (panel b). The broadband 36 Hz peak in panel b has a coherence value of 0.62. The broadband 36 Hz tone might be an entropy-wave feedback tone. This broadband 36 Hz tone does not appear in the unaligned coherence.

The 18 Hz tone and the 354 Hz tones identified using the unaligned coherence are also present in the aligned coherence. The 18 Hz tone has a coherence value of 0.27. The 354 Hz tone might be related to a compressor disk tone.

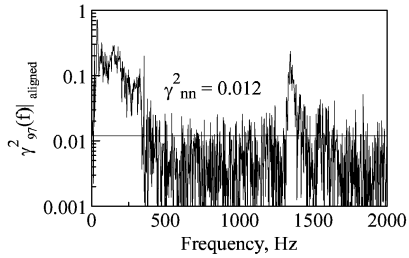

a) 48 percent maximum power

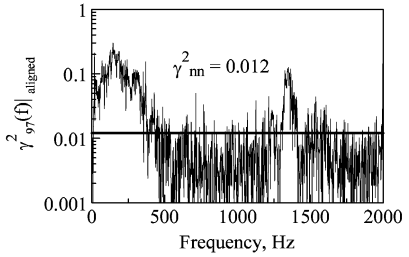

b) 54 percent maximum power

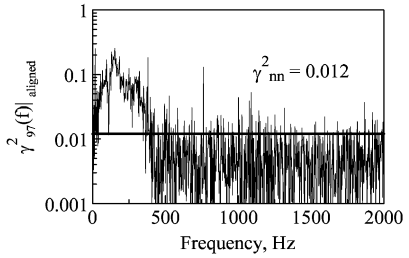

c) 60 percent maximum power

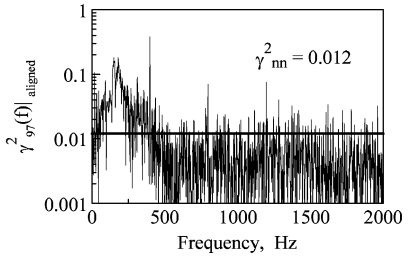

d) 71 percent maximum power

Fig. 11 Aligned unfiltered coherence between microphone at 130° and CIP1 combustor pressure sensor.

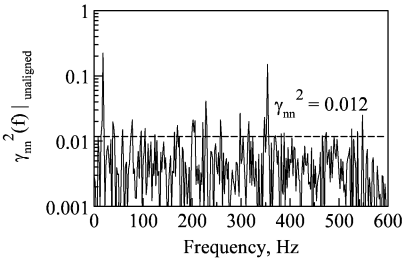

a) 48 percent maximum power

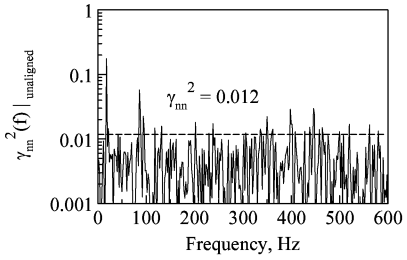

b) 54 percent maximum power

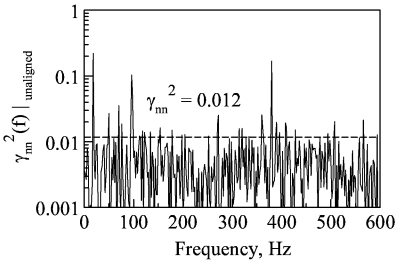

c) 60 percent maximum power

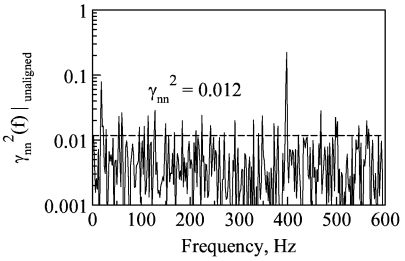

d) 71 percent maximum power

Fig. 12 Deliberately unaligned coherence between microphone at 130° and CIP1 combustor pressure sensor. Signal processing used signals low-pass-filtered at 400 Hz unaligned by 2.74 sample segment lengths ($D_T = 2.74T_d = 1.37$ s) to measure coherence noise floor and to observe tones.

Ignoring the tone, the coherence plots in Figs. 14b and 15b indicate that the combustion noise peaks between 100 and 200 Hz. The coherent output-power plots shown in Figs. 14d and 15d also indicate that the combustion noise peaks between 100 and 200 Hz. Similar results were obtained at engine power settings of 54, 60, and 71% of the maximum power setting.

E. Filtering to Remove Frequencies Greater than 150 Hz

For the 150 Hz low-pass-filtered signal, peak values of the cross-correlation function are shown in Table 7 and occur near 91 ms. These peak values are significantly different from the values obtained using the unfiltered signals and the signals low-pass-filtered at 400 Hz, which are closer to 90 ms.

Figure 16c shows that the phase angle in the 200–400 Hz region (direct noise source region) is flat if a 86.98 time delay is removed. Figure 17c shows that the phase angle in the 0–200 Hz region (indirect noise source region) is flat if a 90.03 ms time delay is removed. This yields a 3.05 ms time delay between the direct combustion noise acoustic signal and the indirect combustion noise acoustic signal.

Figures 16 and 17 show the ripple in the cross-correlation function (panel a) corresponding to the peak in the aligned coherence function near 36 Hz (panel b). The 18 Hz tone identified using the unaligned coherence is also present in the aligned coherence.

Ignoring the tone, the coherence plots in Figs. 16b and 17b again indicate that the combustion noise peaks between 100 and 200 Hz. The coherent output-power plots shown in Figs. 16d and 17d also indicate that the combustion noise peaks between 100 and 200 Hz. Similar results were obtained at engine power settings of 54, 60, and 71% of the maximum power setting.

IV. Discussion

A. Dependent Source Separation

An interpretation of the results shown in Table 7 can be made by plotting the time delays at the peak of the cross correlation of the filtered 130° microphone signal and the CIP1 combustor sensor signal. Let

$$\Delta\tau(f_L)|_{\text{peak}} = \tau(f_L)|_{\text{peak}} - 90 \text{ ms} \tag{6}$$

where the plotting values of the time delays is calculated relative to 90 ms. This plot is shown in Fig. 18. As the low-pass-filter design cutoff frequency f_L is reduced, the time delays tend to increase, because an decreasing amount of direct combustion noise is present. The reference value of 90 ms was selected, since the results of using no filter and a 400 Hz filter are near this value, as is propagation time delay, shown in Table 1. As shown in Fig. 18, the maximum time delay is about 2 ms.

B. Propagation-Time Evaluation Method

Evaluation of the propagation time using the cross spectrum between a combustor pressure sensor and a far-field microphone at 100 ft and 130° as done herein and by Miles [1] indicated that the direct signal had a time delay of 86.98 ms and the indirect signal had a time delay of 90.03 ms. The difference is 3.05 ms, which is attributed to the entropy convecting with the flow before entering the turbine. The linear connection between entropy and pressure fluctuations found by Miles et al. [16] implies that the direct and indirect combustion noise are dependent. The original concept was that the low-frequency core noise source was the combustor and the noise traveled upstream from the combustor through the nozzle. Let the distance the entropy disturbance travels to the turbine entrance be L_c, and let the distance from the turbine entrance to the far field microphone be r. Thus, the direct combustion noise time of travel, τ_d, is

$$\tau_d = 87.2 \text{ ms} = \frac{L_c}{v_s + c_c} + \frac{r}{c_o} \tag{7}$$

Table 9 Tones identified with unaligned coherence (see Fig. 11)

Tone frequency, Hz	Coherence magnitude
48% engine power	
18	0.2228
354	0.15
54% engine power	
18	0.17629
86	0.0574
60% engine power	
18	0.2206
96	0.103
380	0.16848
71% engine power	
18	0785
398	0.2223

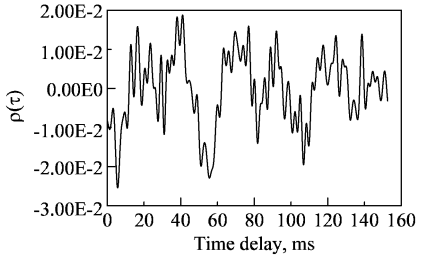

a) 48 percent maximum power

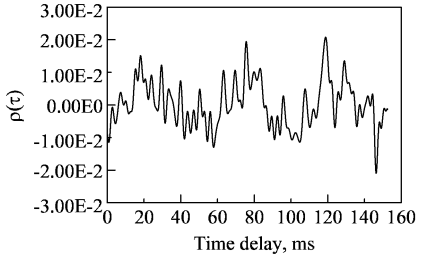

b) 54 percent maximum power

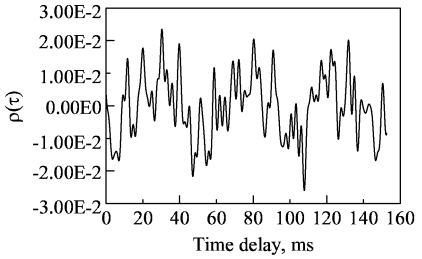

c) 60 percent maximum power

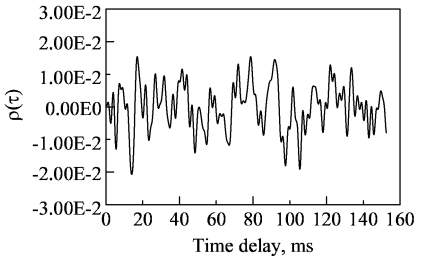

d) 71 percent maximum power

Fig. 13 Deliberately unaligned cross-correlation function between microphone at 130° and CIP1 combustor pressure sensor. Signal processing is done using signals low-pass-filtered at 400 Hz unaligned by 2.74 sample segment lengths ($D_T = 2.74T_d = 1.37$ s) to observe tones.

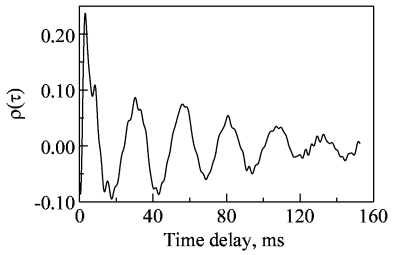

a) Cross-correlation function

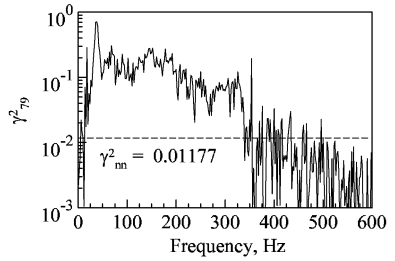

b) Coherence function

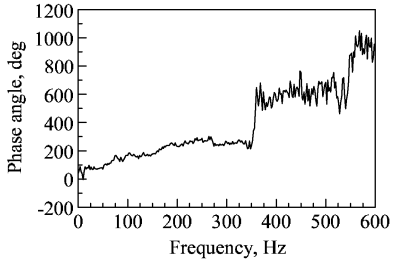

c) Aligned unwrapped cross-spectrum phase angle

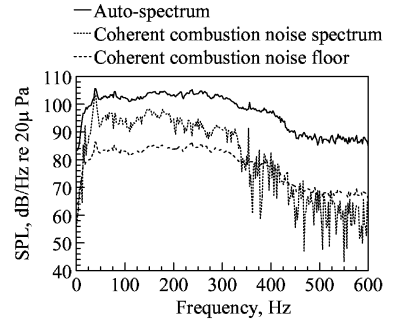

d) Coherent output powerwith a 6 dB ground reflection correction

Fig. 14 Turbofan engine power setting of 48% of maximum power. Microphone at 130°. Signal processing done using aligned signals filtered at 400 Hz ($D_T = 5700/65,536 = 86.98$ ms).

where $L_c = 0.095$ m; $v_s = 30$ m/s; $c_c = 800$ m/s; $r = 30.48$ m; the speed of sound in air is $c_o = 350$ m/s; and the acoustic travel time in the tailpipe, τ_{duct}, is neglected, since it is small and the same for all the sources.

The indirect combustion noise time of travel, τ_i, is

$$\tau_i = 90.11 \text{ ms} = \frac{L_c}{v_s} + \frac{r}{c_o} \tag{8}$$

Consequently,

$$\Delta\tau = \tau_i - \tau_d = 3.052 \text{ ms} = L_c(1/v_s - 1/(v_s + c_c))$$

As dependent time histories, these two sources are separated by the cross-spectrum procedure. However, the separation is not clearly displayed using the cross-correlation method. This time-delay measurement discrepancy is attributed to difficulties in sufficiently separating the mixture of indirect combustion noise in the 0–200 Hz frequency range from the direct combustion noise in the 200–400 Hz frequency range. This problem can be seen in Figs. 16 and 17, in which results of using the 150 Hz low-pass-filtered signals with the cross-spectrum method are presented. The use of a time delay of 86.98 ms creates a flat phase angle between 200–300 Hz, shown in Fig. 15c, indicating that this is the direct combustion noise location, whereas using a time delay of 90.03 ms creates flat phase angle between 0–200 Hz, shown in Fig. 16c, indicating this is the indirect combustion noise location. Using this 150 Hz low-pass filter still leaves the signals intermixed so that one is able to distinguish between direct and indirect combustion noise. In addition, as the low-pass-filter frequency is reduced, the cross-correlation peaks in the time domain get wider. As a consequence, low-pass filtering is not as useful as one would hope in revealing the direct combustion noise.

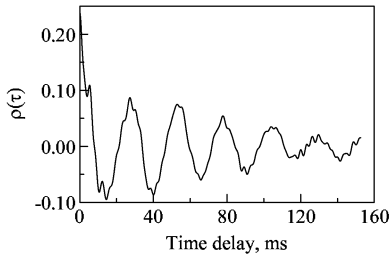

a) Cross-correlation function

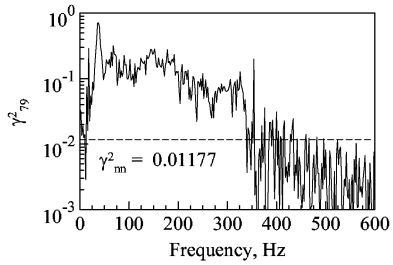

b) Coherence function

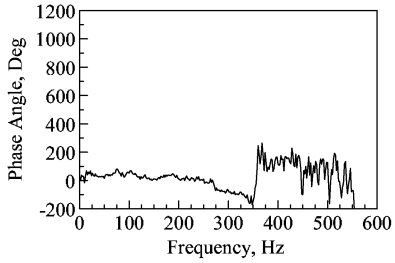

c) Aligned unwrapped cross-spectrum phase angle

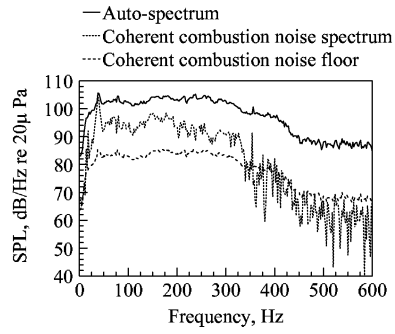

d) Coherent output power with a 6 dB ground reflection correction

Fig. 15 Turbofan engine power setting of 48% of maximum power. Microphone at 130°. Signal processing done using aligned signals filtered at 400 Hz ($D_T = 5900/65,536 = 90.03$ ms).

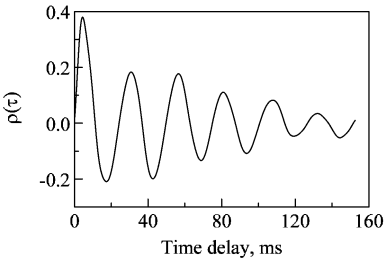

a) Cross-correlation function

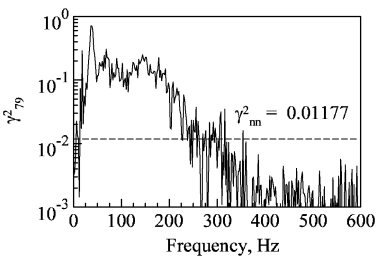

b) Coherence function

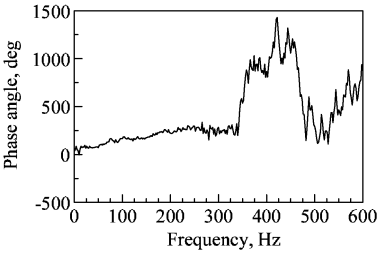

c) Aligned unwrapped cross-spectrum phase angle

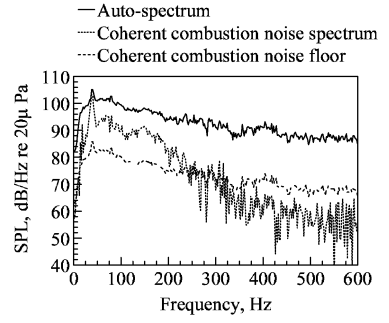

d) Coherent output power with a 6 dB ground reflection correction

Fig. 16 Turbofan engine power setting of 48% of maximum power. Microphone at 130°. Signal processing done using aligned signals filtered at 150 Hz ($D_T = 5700/65,536 = 86.98$ ms).

However, these results do show that low-pass filtering can be used with the cross-correlation function to separate this type of dependent source to some extent and confirm the cross-spectrum results.

C. Identification of Combustion Noise

The use of a sequence of low-pass filters to study the cross correlation of the noise from the CIP1 sensor and the 130° far-field microphone also shows that filtering can increase the correlation function significantly. The peak values of the correlation function shown in Table 8 are plotted in Fig. 19. A low-pass filter in the range of 200–300 Hz works well. Also note that when a tone is present, as it is for the 48% of maximum power setting, the correlation is increasing, because the tone becomes increasingly dominant.

D. Identification of Periodic Components

For an engine power setting 48% maximum power a strong periodic signal is revealed by the cross-correlation function calculated using the far-field microphone and the combustor sensor. This signal appears with or without filtering, as shown in Fig. 3. The coherence shown in Figs. 14b, 15b, 16b, and 17b and the coherent output power shown in Figs. 14d, 15d, 16d, and 17d also indicate the presence of this rumble. The cross-correlation function indicates that the rumble has period of about $T = 0.025$ s, which means that the frequency is about $f = 1/T = 40$ Hz, as shown. This rumble corresponds to the 36 Hz peak observable in the aligned coherence plots shown in Figs. 14b, 15b, 16b, and 17b. This rumble is not a tone, since a strong tone signal at this frequency is not observable in Fig. 12a. The signal may be due to a feedback mechanism. At a higher power setting, it is not observed.

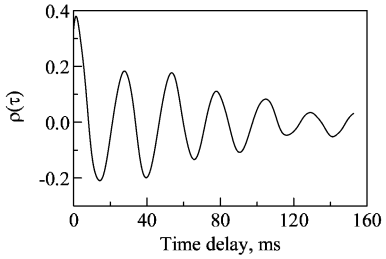

a) Cross-correlation function

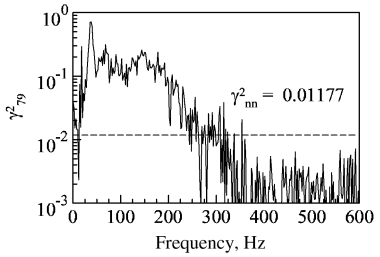

b) Coherence function

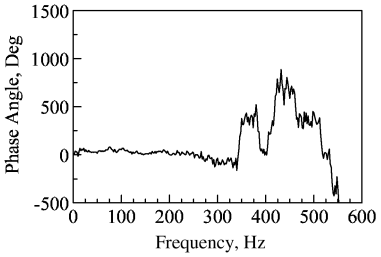

c) Alignedun wrapped cross-spectrum phase angle

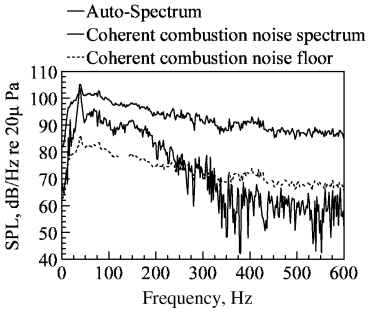

d) Coherent output power

Fig. 17 Turbofan engine power setting of 48% of maximum power. Microphone at 130°. Signal processing done using aligned signals filtered at 150 Hz ($D_T = 5900/65,536 = 90.03$ ms).

A somewhat similar cross-correlation function was shown in Fig. 13 of a study by Reshotko and Karchmer [28] of combustion noise from a Pratt & Whitney JT15D with 40% maximum power. The cross-correlation function had a period of about $T = 0.07$ s, which indicates a frequency of about $f = 1/T = 142$ Hz. This corresponded to the peak of the largest coherence function shown in Fig. 14 of the paper by Reshotko and Karchmer [28].

The cross-correlation function identifies periodic components in a manner that clearly indicates their significance.

E. Source Separation

The cross-correlation function of white noise and white noise displaced by 86.98 ms, as shown in Fig. 2, produces a spike at 86.98 ms. Close examination shows some structure to the function with features that vary positively and negatively by 10^{-4} and 10^{-5}.

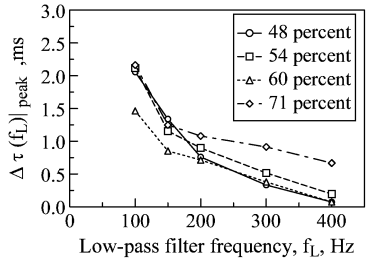

Fig. 18 Time delay at peak value of cross-correlation function of low-pass-filtered signals as a function of filter design frequency f_L less 90 ms.

For filtered white noise, the cross-correlation function is no longer sharp, as shown in Fig. 2. The resolution has been decreased by filtering. The presence of tones creates new issues, as shown in Fig. 3.

The plots shown in Figs. 3–9 show that two separate peaks cannot always be observed in the cross-correlation function.

Source separation of direct and indirect combustion noise cannot always be reliably determined directly from the cross correlation. However, a time delay was identified in all cases by the cross-correlation function, clearly indicating the combustor as the source of the noise. In addition, using different low-pass-filter cutoff frequencies clearly separates the sources. The cross-correlation function peaks at a time delay depending on the blend of indirect and direct combustion noise. The unfiltered signals and the signals low-pass-filtered at 400 Hz have time delays that peak at about 90 ms. The signals low-pass-filtered at 150 Hz have time delays that peak at about 91 ms.

These results suggest that previous discussions of the measurements of the cross correlation between the combustor and a far-field microphone by Karchmer and Reshotko [26], Karchmer [27], Reshotko and Karchmer [28], and Mathews et al. [29] did not consider that the measured time delay using filtered signals was caused by a blend of signals from direct and indirect combustion noise. Consequently, these previous measurements might be due more to indirect combustion noise than direct combustion noise, because filtered cross-correlation functions are used by Karchmer and Reshotko [26], Karchmer [27], Reshotko and Karchmer [28], and Mathews et al. [29], and some of the direct combustion noise may have been removed by filtering.

The cross-correlation-function and coherence-function methods provide a procedure to detect the presence of coherent indirect and direct combustion noise when both are present. However, the inherent smearing in the filtering renders it difficult to determine the relative contribution of indirect and direct combustion noise to the total combustion noise.

F. Combustor Acoustic Measurements

The low-frequency acoustic cross spectrum and the acoustic cross-correlation function have been identified for a range of operating conditions. The circumferential acoustic combustor modes in the TECH977 engine are discussed by Royalty and Schuster [6]. They found that most of the acoustic energy below 500 Hz is contained in the plane-wave mode (mode order of 0). The results presented

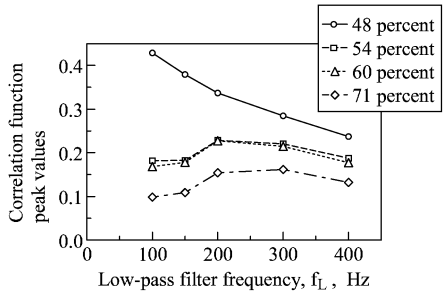

Fig. 19 Peak values of low-pass-filtered cross-correlation function as a function of filter design frequency f_L.

correspond to the propagation of plane waves from the combustor to the far field.

G. Limitations

The presence of tones in the signals and the decrease in resolution of the cross-correlation function with the filtering prevented the cross-correlation function from identifying source separation of direct and indirect combustion noise by finding separate time delays for each. These limitations were overcome to some extent by using the low-pass-filter approach. However, the presence of low-frequency tones in the filter band remains a problem.

The cross-spectrum phase-angle approach identifies the indirect combustion noise propagation time to be of the order of 90 ms, and the correlation-function approach identifies the indirect combustion noise propagation time to be of the order of 91–92 ms. The cross-spectrum phase-angle approach identifies the direct combustion noise propagation time to be of the order of 87 ms, and the correlation-function approach identifies the direct combustion noise propagation speed to be less than 90 ms.

The lowest cutoff frequency filter removes much of the random broadband noise. However, this creates signals with a correlation strongly influenced by the remaining tones. This makes it difficult to obtain a valid propagation time delay for the indirect combustion noise in the 0–200 Hz frequency band.

A 200–400 Hz bandpass filter was used in hopes of identifying a better time delay for the direct combustion noise in this frequency band. However, the resulting correlation function did not have a single identifiable peak. In place of the peak was a modulated waveform with many peaks that appeared in the 80–100 ms region with an envelope that had a single peak in the region. Discussing the use of sophisticated notch and bandpass filters to analyze this data is beyond the scope of this paper.

The correlation-function procedure currently supplies support for the idea that the indirect and direct core noise can be separated by the time delay due to entropy-wave (hot-spot) convection. However, the method for this data set does not produce the same result as that given by examination of the cross-spectrum phase angle; in addition, it is more complicated to apply. The best part about the correlation-function procedure is that it gives definite evidence that combustion noise is part of the far-field signal.

H. Delay-Time Consistency

Table 7 shows that the delay times measured are more dependent on the filtering than on the operating condition. This can be understood in general terms using information from papers on gas-turbine engine instability, such as those in a volume edited by Lieuwen and Yang [39], with information on gas-turbine combustion, as discussed by Lefebvre [53], and with information from Hill and Peterson [37] on the mechanics and thermodynamics of propulsion.

It is assumed that the delay time only depends on the difference between the travel time of the entropy to the turbine and the acoustic travel time to the turbine. From the turbine to the far field, the signals are acoustic and travel the same path to the far-field microphone. In calculating the noise produced by a hot spot, one might have to consider which blade produced the noise and the further propagation of a hot spot. These complications will be ignored.

The delay time can be estimated by

$$\Delta\tau = \tau_s - \tau_a \approx L_c/v_s - L_c/c_c = (L_c/c_c)(1/M_c - 1)$$
$$= (L_c/c_c)(1 - M_c)/M_c \approx L_c/v_s \tag{9}$$

where $M_c = v_s/c_c$ is the combustor Mach number, and $c_c = \sqrt{\gamma \Re T_c/W}$ is the local speed of sound in the combustor.

The difference in the measured time delay for the direct combustion noise and the indirect combustion noise, $\Delta\tau$, has been shown to be about 3 ms using the method based on the cross-spectrum phase angle. The use of the correlation-function approach yielded a mixed value of $\Delta\tau$ of the order of 2 to 5 ms. Reasonable values of L_c, T_c, and M_c yield a value of 2 to 5 ms for $\Delta\tau$. However, this must be left as an exercise for the reader.

The interesting point about Eq. (9) is that the delay time is mainly established by the combustor flow velocity and combustor length. Consequently, whatever the actual combustor length and whatever the combustor Mach number, over a range of engine operating conditions, the time delay measured by the cross-correlation function should be fairly constant.

V. Conclusions

Unfiltered and low-pass-filtered cross-correlation functions between a combustor pressure sensor and a far-field microphone at 130° at the 54, 60, and 71% maximum power settings showed a single time-delay peak. However, at the 48% maximum power setting, a single or double peak was observed depending on the low-pass-filter cutoff frequency. The 48% operating condition cross-correlation functions showed a double peak when using signals unfiltered and filtered with cutoff frequencies of 400, 300, and 200 Hz. For the unfiltered cross-correlation and the cross correlation filtered using a 400 Hz cutoff frequency at each power setting, the largest peak is at an acoustic time delay near 90 ms. For the double-peak case at the 48% operating condition, the second peak is near 95 ms. This indicates that the left side of the double peak or single peak is due to direct combustion noise, which travels at acoustic speeds over its total path length; the right side of the double peak or single peak is due to indirect combustion noise.

Low-pass filtering with a 100 Hz cutoff frequency to remove a large amount of the direct combustion noise leaves the indirect combustion noise, which has approximately a 92 ms time delay. This time delay is longer than the time delay observed with no filtering or low-pass filtering at 400 Hz, which produced a time delay near 90 ms. This shows that some of the direct combustion noise, which is always traveling at the speed of sound, has been removed, leaving the indirect combustion noise, which spends time moving convectively at a much lower velocity than the speed of sound in the combustor. As a consequence of removing part of the combustion noise that travels fastest, the delay time of the combustion noise remaining in the signal is greater. The largest indirect combustion noise time delay found using this procedure is about 2 ms. The cross-correlation function, when used with low-pass filtering, is very useful in separating the indirect and direct combustion noise sources in this system.

Coherence analysis using the cross-spectrum phase-angle method separates direct and indirect combustion noise using filtered or unfiltered signals. This is done by an examination of the effect that use of different time delays has on the phase angle of the cross spectrum calculated using the combustor pressure-sensor signal and a far-field microphone signal. For the cross spectrum between a combustor pressure sensor and a far-field microphone at 130°, this method indicated that the direct signal had a time delay of 86.98 ms and the indirect signal had a time delay of 90.03 ms. The indirect combustion noise time-delay time is thus 3.05 ms. This time-delay measurement discrepancy is attributed to difficulties in sufficiently separating the mixture of indirect combustion noise in the 0–200 Hz frequency range from the direct combustion noise in the 200–400 Hz frequency range. In addition, as the low-pass-filter frequency is reduced, the cross-correlation peaks in the time domain get wider. These results show that low-pass filtering can be used with the cross-correlation function to separate this type of dependent source to some extent and confirm the cross-spectrum results. These results are based on a set of static engine tests conducted for one specific dual-spool turbofan engine configuration. However, they may lead to a better idea about the acoustics in the combustor turbine-tailpipe system and may help develop and validate improved reduced-order physics-based methods for predicting turbofan engine core noise.

References

[1] Miles, J. H., "Spectral Separation of the Turbofan Engine Coherent Combustion Noise Component," AIAA Paper 2008-50, Jan. 2008; also NASA TM-215157-0, 2008.

[2] Miles, J. H., "Time Delay Analysis of Turbofan Engine Direct and Indirect Combustion Noise Sources," *Journal of Propulsion and Power*, Vol. 25, No. 1, Jan.–Feb. 2009, pp. 218–227. doi:10.2514/1.38030
[3] Mendoza, J. M., Nance, D. K., and Ahuja, K. K., "Source Separation from Multiple Microphone Measurements in the Far Field of a Full Scale Aero Engine," AIAA Paper 2008-2809, 2008.
[4] Weir, D. S., and Mendoza, J. M., "Baseline Noise Measurements from the Engine Validation of Noise and Emissions Reduction Technology Program," AIAA Paper 2008-2807, 2008.
[5] Schuster, B., "Statistical Considerations for Gas Turbine Engine Noise Measurements," AIAA Paper 2008-2808, 2008.
[6] Royalty, C. M., and Schuster, B., "Noise fro a Turbofan Engine Without a Fan from the Engine Validation of Noise and Emission Reduction Technology (EVNERT) Program," AIAA Paper 2008-2810, 2008.
[7] Dougherty, R. P., and Mendoza, J. M., "Nacell In-duct Beamforming Using Modal Steering Vectors," AIAA Paper 2008-2812, 2008.
[8] Weir, D. S., "Engine Validation of Noise and Emission Reduction Technology Phase 1," NASA CR-2008-215225, May 2008.
[9] Hultgren, L., and Miles, J., "Noise-Source Separation Using Internal and Far-Field Sensors for a Full-Scale Turbofan Engine," 15th AIAA/CEAS Aeroacoustics Conference, AIAA Paper 2009-3220, Miami, FL, May 2009.
[10] Pickett, G. F., "Core Engine Noise Due to Temperature Fluctuating Through Turbine Blade Rows," AIAA Paper 75-528, 1975.
[11] Cumpsty, N. A., and Marble, F. E., "The Interaction of Entropy Fluctuations with Turbine Blade Rows; A Mechanism of Turbojet Noise," *Proceedings of the Royal Society of London A*, Vol. 357, 1977, pp. 323–344. doi:10.1098/rspa.1977.0171
[12] Cumpsty, N. A., and Marble, F., "Core Noise from Gas Turbine Exhausts," *Journal of Sound and Vibration*, Vol. 54, No. 2, 1977, pp. 297–309. doi:10.1016/0022-460X(77)90031-1
[13] Cumpsty, N. A., "Jet Engine Combustion Noise: Pressure, Entropy and Vorticity Perturbations Produced by Unsteady Combustion or Heat Addition," *Journal of Sound and Vibration*, Vol. 66, No. 4, 1979, pp. 527–544. doi:10.1016/0022-460X(79)90697-7
[14] Gliebe, P., Mani, R., Shin, H., Mitchell, B., Ashford, G., Salamah, S., and Connell, S., "Acoustic Prediction Codes," NASA CR–2000-210244, Aug. 2000.
[15] Mani, R., "Issues in Combustion Noise," *Annual Research Briefs 2007*, Stanford Univ., Center for Turbulence Research, Stanford, CA, 2007, pp. 255–264, http://ctr.stanford.edu/ResBriefs07/22_mani_pp255_264.pdf [retrieved Nov. 2009].
[16] Miles, J. H., Wasserbauer, C. A., and Krejsa, E., "Cross Spectra Between Temperature and Pressure in a Constant Area Duct Downstream of a Combustor," AIAA Paper 83-0762, 1983; also NASA TM-83351, 1983.
[17] Bendat, J. S., and Piersol, A. G., *Measurement and Analysis of Random Data*, Wiley, New York, 1966.
[18] Bendat, J. S., and Piersol, A. G., *Random Data: Analysis and Measurement Procedures*, Wiley, New York, 1971.
[19] Bendat, J. S., and Piersol, A. G., *Engineering Applications of Correlation and Spectral Analysis*, Wiley, New York, 1980.
[20] Childers, D., and Durling, A., *Digital Filtering and Signal Processing*, West Publishing, St. Paul, MN, 1975.
[21] Kay, S. M., *Modern Spectral Estimation*, Prentice–Hall, Upper Saddle River, NJ, 1987.
[22] Stearns, S. D., and David, R. A., *Signal Processing Algorithms Using Fortran and C*, Prentice–Hall, Upper Saddle River, NJ, 1993.
[23] Candy, J. V., *Signal Processing: The Modern Approach*, McGraw–Hill, New York, 1988, pp. 108–111.
[24] Lee, Y. W., Cheatham, T. P., Jr., and Wiesner, J. B., "Application of Correlation Analysis to the Detection of Periodic Signals in Noise," *Proceedings of the IRE*, Vol. 39, No. 9, Sept. 1951, pp. 1094–1096. doi:10.1109/JRPROC.1951.273757
[25] White, P. H., "Cross Correlation in Structural Systems: Dispersion and Nondispersion Waves," *Journal of the Acoustical Society of America*, Vol. 45, No. 5, 1969, pp. 1118–1128. doi:10.1121/1.1911582
[26] Karchmer, A. M., and Reshotko, M., "Core Noise Source Diagnostics on a Turbofan Engine Using Correlation and Coherence Techniques," NASA TMX-73535, 1976.
[27] Karchmer, A. M., "Identification and Measurement of Combustion Noise from a Turbofan Engine Using Correlation and Coherence Techniques," NASA TM-73747, 1977; also Ph.D. Thesis, Dept. of Mechanical and Aerospace Engineering, Case Western Reserve Univ., Cleveland, OH.
[28] Reshotko, M., and Karchmer, A., "Core Noise Measurements from a Small, General Aviation Turbofan Engine," NASA TM-81610, 1980.
[29] Mathews, D. C., Rekos, N. F., Jr., and Nagel, R. T., "Combustion Noise Investigation," Federal Aviation Administration Rept. FAA-RD-77-3, 1977.
[30] Shivashankara, B. N., "Gas Turbine Core Noise Source Isolation by Internal-to-Far-Field Correlations," *Journal of Aircraft*, Vol. 15, No. 9, Sept. 1978, pp. 597–600. doi:10.2514/3.58412
[31] Harper-Bourne, M., Moore, A., and Siller, H., "A Study of Large Aero-Engine Combustor Noise," AIAA Paper 2008-2942, May 2008.
[32] Schemel, C., Thiele, F., Bake, F., Lehmann, B., and Michel, U., "Sound Generation in the Outlet Section of Gas Turbine Combustion Chambers," AIAA Paper 2004-2929, 2004.
[33] Richter, C., Panek, L., and Thiele, F. H., "On the Application of CAA-Methods for the Simulation of Indirect Combustion Noise," AIAA Paper 2005-2919, May 2005.
[34] Bake, F., Michel, U., Rohle, I., Richter, C., Thiele, F., Liu, M., and Noll, B., "Indirect Combustion Noise Generation in Gas Turbines," AIAA Paper 2005-2830, May 2005.
[35] Bake, F., Michel, U., and Roehle, I., "Investigation of Entropy Noise in Aero-Engine Combustors," *Journal of Engineering for Gas Turbines and Power*, Vol. 129, April 2007, pp. 370–376. doi:10.1115/1.2364193
[36] Bake, F., Kings, N., and Roehle, I., "Fundamental Mechanism of Entropy Noise in Aero-Engines: Experimental Investigation," *Journal of Engineering for Gas Turbines and Power*, Vol. 130, No. 1, Jan. 2008, Paper 011202. doi:10.1115/1.2749286
[37] Hill, P. G., and Peterson, C. R., *Mechanics and Thermodynamics of Propulsion: Second Edition*, Addison-Wesley, Reading, MA, 1992.
[38] Poinsot, T., and Veynante, D., *Theoretical and Numerical Combustion*, 2nd ed., Edwards, Philadelphia, 2005.
[39] Lieuwen, T. C. and Yang, V. (eds.), *Combustion Instabilities in Gas Turbine Engines: Operational Experience, Fundamental Mechanisms, and Modeling*, AIAA, Reston, VA, 2005.
[40] Barrett, E. W., and Suomi, V. E., "Preliminary Report on Temperature Measurement by Sonic Mean," *Journal of Meteorology*, Vol. 6, Aug. 1949, pp. 273–276.
[41] Cramer, O., "The Variation of the Specific Hear Ratio and the Speed of Sound in Air with Temperature, Pressure, Humidity, and CO_2 Concentration," *Journal of the Acoustical Society of America*, Vol. 93, No. 5, May 1993, pp. 2510–2516. doi:10.1121/1.405827
[42] Knapp, C. H., and Carter, G. C., "The Generalized Correlation Method for Estimation of Time Delay," *IEEE Transactions on Acoustics, Speech, and Signal Processing*, Vol. 24, No. 4, 1976, pp. 320–327. doi:10.1109/TASSP.1976.1162830
[43] Carter, G. C., "Tutorial Overview of Coherence and Time Delay Estimation," *Coherence and Time Delay Estimation*, edited by G. C. Carter, Chap. Pt. 1, IEEE Press, New York, 1993, pp. 1–27.
[44] Scarbrough, K., Ahmed, N., and Carter, G. C., "On the Simulation of a Class of Time Delay Estimation Algorithms," *IEEE Transactions on Acoustics, Speech, and Signal Processing*, Vol. 29, No. 3, Pt. 2, June 1981, pp. 534–540. doi:10.1109/TASSP.1981.1163615
[45] Kormylo, J. J., and Jain, V. K., "Two-Pass Recursive Digital Filter with Zero Phase Shift," *IEEE Transactions on Acoustics, Speech, and Signal Processing*, Vol. 22, No. 5, Oct. 1974, pp. 384–387. doi:10.1109/TASSP.1974.1162602
[46] Hamming, R. W., *Digital Filters Third Edition*, Dover, Mineola, NY, 1989, p. 252.
[47] Matsumoto, M., and Nishimura, T., "Mersenne Twister: a 623-Dimensionally Equidistributed Uniform Pseudo-Random Number Generator," *ACM Transactions on Modeling and Computer Simulation*, Vol. 8, No. 1, Jan. 1998, pp. 3–30. doi:10.1145/272991.272995
[48] Carter, G. C., "Coherence and Time Delay Estimation," *Proceedings of the IEEE*, Vol. 75, No. 2, Feb. 1987, pp. 236–255. doi:10.1109/PROC.1987.13723
[49] Carter, G. C., "Receiver Operating Characteristics for a Linearly Thresholded Coherence Estimation Detector," *IEEE Transactions on Acoustics, Speech, and Signal Processing*, Vol. 25, Feb. 1977, pp. 90–92. doi:10.1109/TASSP.1977.1162898

[50] Halliday, D. M., Rosenberg, J. R., Amjad, A. M., Breeze, P., Conway, B. A., and Farmer, S. F., "A Framework for the Analysis of Mixed Time Series/Point Process Data-Theory and Application to the Study of Physiological Tremor, Single Motor Unit Discharges and Electromyograms," *Progress in Biophysics and Molecular Biology*, Vol. 64, No. 2, 1995, pp. 237–278.
doi:10.1016/S0079-6107(96)00009-0

[51] Brillinger, D. R., *Time Series Data Analysis and Theory*, Holden-Day, San Francisco, 1981.

[52] Miles, J. H., "Aligned and Unaligned Coherence: A New Diagnostic Tool," 44th AIAA Aerospace Science Meeting, Reno, NV, AIAA Paper 2006-0010, 2006; also NASA TM-2006-214112.

[53] Lefebvre, A. H., *Gas Turbine Cobustion*, Taylor & Francis, London, 1999.

K. Frendi
Associate Editor